Available online at www.sciencedirect.com

ScienceDirect

European Journal of Protistology 60 (2017) 119–133

European Journal of PROTISTOLOGY

www.elsevier.com/locate/ejop

# Morphologic and phylogenetic studies of two hypotrichous ciliates, with notes on morphogenesis in *Gastrostyla steinii* Engelmann, 1862 (Ciliophora, Hypotrichia)

Xiaotian Luo[a,d,1], Lifang Li[b,c,1], Chundi Wang[a], William Bourland[d], Xiaofeng Lin[e,*], Xiaozhong Hu[a,*]

[a] *Institute of Evolution and Marine Biodiversity, Ocean University of China, Qingdao 266003, China*
[b] *Marine College, Shandong University, Weihai 264209, China*
[c] *Department of Biological Sciences, University of Ulsan, Ulsan 44610, Korea*
[d] *Department of Biological Sciences, Boise State University, Boise 83725, USA*
[e] *Guangzhou Key Laboratory of Subtropical Biodiversity and Biomonitoring, School of Life Science, South China Normal University, Guangzhou 510631, China*

Received 27 December 2016; received in revised form 24 April 2017; accepted 2 May 2017
Available online 17 May 2017

## Abstract

Two oxytrichid ciliates, *Stylonychia* (*Metastylonychia*) *nodulinucleata* Shi and Li, 1993 and *Gastrostyla steinii* Engelmann, 1862; collected from Huguangyan Maar Lake and Shenzhen Mangrove Nature Protection Area, southern China, respectively, were investigated using standard methods. The uncommon species *Stylonychia* (*Metastylonychia*) *nodulinucleata* can be recognized by its large body size, the conspicuous caudal cirri in vivo, and a moniliform macronucleus. We provide the first record of the small subunit ribosomal RNA (SSU rRNA) gene sequence for the species. The division of *Stylonychia* into two subgenera based on morphological and morphogenetic data is supported by the phylogenetic analyses, in which *Stylonychia* (*Metastylonychia*) *nodulinucleata* is placed as a sister branch to the clade including all the sequences of *Stylonychia* (*Stylonychia*) *mytilus* complex. The first brackish water population of *Gastrostyla steinii* is described in detail, with emphasis on its morphogenesis, which corresponds well with previous populations. In the phylogenetic trees, all the available *Gastrostyla* sequences, except for *Gastrostyla* sp. Y2 (KT780432) (probably a misidentification), nest together in the big group of the subfamily Stylonychinae with moderate to high support (ML/BI, 91%/0.95), very likely revealing the monophyly of the genus *Gastrostyla*.


***Keywords:*** Classification; Ontogenesis; Oxytrichid ciliates; Redescription; SSU rRNA; *Stylonychia* (*Metastylonychia*) *nodulinucleata*

## Introduction

The Oxytrichidae Ehrenberg, 1830 is one of the largest groups within the Spirotrichea Bütschli, 1889. Comprising more than 200 described species, it is a highly diverse family with respect to morphological and ontogenetic patterns (e.g. Berger 1999, 2011; Foissner 2016; Foissner et al. 2002; Shao

*Corresponding authors.
*E-mail addresses:* xlin@scnu.edu.cn (X. Lin), xiaozhonghu@ouc.edu.cn (X. Hu).
[1] Co-first authors.

http://dx.doi.org/10.1016/j.ejop.2017.05.001
0932-4739/

et al. 2015; Song et al. 2009). Recently, this group has been proven to be much more diverse than originally supposed, largely as a result of faunistic investigations of new habitats (e.g. Chen et al. 2015; Fan et al. 2015; Foissner 2016; Hu and Kusuoka 2015; Jung et al. 2015; Kumar et al. 2015; Lu et al. 2015; Shao et al. 2011, 2014a, 2014b; Singh and Kamra 2015; Singh et al. 2013; Wang et al. 2016). The oxytrichid genus *Stylonychia* was established by Ehrenberg (1830) with *S. mytilus* designated as the type species by Fromentel (1875). So far, 12 valid species have been assigned to it, of which only *Stylonychia nodulinucleata* Shi and Li, 1993 has a moniliform macronucleus (Berger 1999, 2001; Eigner 1997, 1999; Foissner 2016; Gupta et al. 2001; Kumar and Foissner 2017; Shi and Ammermann 2004). Another oxytrichid genus, *Gastrostyla*, with more than 18 frontal-ventral-transverse cirri, was established by Engelmann (1862) with *G. steinii*, from the so-called Diebesgraben in Bonn, Germany, as the type. Subsequently, *G. steinii* was isolated and redescribed from various freshwater and/or terrestrial habitats worldwide, possibly excepting the polar region, and there is no brackish water record available substantiated by detailed morphological data (Berger 1999; Foissner et al. 2002). Here, we give a first record for *Gastrostyla steinii* from a Chinese brackish water body with the original salinity of 15‰, and supply a detailed description of its morphogenesis.

In this work, we also describe the morphology and SSU rRNA gene sequence of *Stylonychia nodulinucleata*. Phylogenetic analyses based on SSU rRNA gene sequences were also made to reveal the systematic position of the two species.

## Material and Methods

### Sample collection, observation and terminology

Samples containing *Stylonychia nodulinucleata* were collected from a freshwater lake, Huguangyan Maar Lake (temperature 20.0 °C; pH 8.3), in Zhanjiang (21°09′21″N; 110°17′28″E), southern China on November 5, 2013. Investigations for *S. nodulinucleata* were made from specimens of raw cultures, that is, not from cloned individuals. However, its body shape, distinct caudal cirri, and a moniliform macronucleus reasonably exclude admixture of related species.

Samples containing *Gastrostyla steinii* were collected from a mixture of water and sediments with organic debris found in a small puddle (temperature 21.3 °C; pH 7.4) in Shenzhen Mangrove Nature Protection Area (22°31′53″N; 114°00′36″E), southern China on November 22, 2015. *Gastrostyla steinii* was recovered from the samples at a salinity of 5‰, with an original salinity of 15‰ (*Gastrostyla steinii* appeared during the cultivation experiments of tolerance of salinity for *Euplotes parawoodruffi*). Studies for *Gastrostyla steinii* were from clonal cultures, which were maintained in Petri dishes at about 25 °C for several weeks, using mineral water (freshwater) with rice grains to enrich the growth of bacterial food for the ciliates.

Living cells were observed and measured using bright field and differential interference contrast microscopy at 40–1000× magnification. Protargol staining according to Wilbert (1975) was used to reveal the infraciliature and nuclear apparatus. This method led to inflation of the stained cells. Counts and measurements on stained specimens were performed at a magnification of 1000× with an ocular micrometer. Drawings were made with the help of a drawing attachment and photomicrographs. In dividers, parental cirri are shown as outlines and newly formed ones are shown as filled outlines. Terminology is according to Berger (1999) and Foissner et al. (2002).

### Amplification of DNA and molecular phylogenetic analyses

One to several cells were washed four times in filtered (0.22 μm) habitat water using a micropipette, and then transferred to a 1.5 mL microfuge tube with a minimum volume of water. Genomic DNA was extracted using the DNeasy Blood & Tissue Kit (Qiagen, CA) according to the manufacturer's instructions. Amplification and sequencing of the SSU rRNA gene were performed according to Zhao et al. (2015). The SSU rRNA gene was amplified by PCR with primers 18S-F (5′-AACCTGGTTGATCCTGCCAGT-3′) and 18S-R (5′-TGATCCTTCTGCAGGTTCACCTAC-3′) (Medlin et al. 1988). The PCR product was sequenced directly in both directions using primers 18S-F, 18S-R and three internal primers (Wang et al. 2016) at Sunny Biotechnology (Shanghai, China).

We selected a set of 82 SSU rRNA gene sequences downloaded from the National Center for Biotechnology Information (NCBI) Database to construct phylogenetic trees. Four oligotrichous ciliates were selected as outgroup taxa, and NCBI accession numbers are given after the species names in the phylogenetic tree (Fig. 7). Ten urostylids selected are as follows: *Apobakuella fusca* (JN008942), *Bergeriella ovata* (FJ754026), *Diaxonella pseudorubra* (GU942564), *Hemicycliostyla sphagni* (FJ361758), *Monocoronella carnea* (FJ775726), *Nothoholosticha fasciola* (FJ377548), *Pseudokeronopsis flava* (DQ227798), *Pseudourostyla cristata* (FJ598608), *Uroleptopsis citrina* (FJ870094), and *Urostyla grandis* (AF164129). All sequences were aligned in GUIDANCE and ambiguous columns in the alignment were removed with default parameters (below 0.93) using the GUIDANCE web server with the MUSCLE alignment algorithm (Edgar 2004; Sela et al. 2015). The resulting alignment was manually edited by removing both primers using the program BIOEDIT 7.2.5 (Hall 1999). The final alignment used for phylogenetic analyses included 1759 sites and 82 taxa. Maximum likelihood (ML) analysis, with 1000 bootstrap replicates, was carried out using RAxML-HPC2 on XSEDE v. 8.2.9 (Stamatakis et al. 2008) on the CIPRES Science Gateway (URL: http://www.phylo.org/sub_sections/portal)

(Miller et al. 2010). The DNA partition was analyzed with GTR + gamma (Gao et al. 2016). The program MrModeltest v.2.0 (Nylander 2004) selected the GTR + I + G (general time reversible + invariable sites + gamma) as the best model with Akaike Information Criterion (AIC), which was then used for Bayesian inference (BI) analysis. BI analysis was performed with MrBayes 3.2.6 on XSEDE (Ronquist et al. 2012), with 1,000,000 generations, a sampling frequency of 100, and a burn-in of 2500 trees. The remaining trees were used to calculate the posterior probabilities with a majority-rule consensus. According to Hillis and Bull (1993), bootstrap values <70% were considered as low, 70–94% as moderate, and ≥95% as high support. For posterior probabilities, values <0.70 were considered as low, 0.70–0.94 as moderate, and ≥0.95 as high support (Alfaro et al. 2003). Tree topologies were visualized using SeaView v 4.6.1 (Gouy et al. 2010) and MEGA 6.0 (Tamura et al. 2013). The systematic classification follows Berger (1999), Eigner (1997, 1999), Lynn (2008) and Adl et al. (2012).

## Results

### *Stylonychia nodulinucleata* Shi and Li, 1993 (Fig. 1A–C, Fig. 2A–P, Table 1)

#### Morphology of the Chinese population

Cell size in vivo 180–240 × 80–110 μm (n = 6). Body rigid, outline obovate, with anterior end broadly rounded or obliquely truncate, posterior end rounded and narrower than anterior end, widest at middle of buccal field. Right margin slightly to distinctly convex, left margin usually concave at mid-body (Figs. 1 A, 2 A–C). Dorsoventrally flattened about 2:1, anterior and posterior quarter of cell thin and hyaline, dorsal side frequently convex, ventral side almost flattened (Fig. 2D). Macronucleus moniliform, composed of four to eleven, usually eight, macronuclear nodules connected by fine strand, arranged like a question mark, individual nodules globular to ellipsoid, or even sausage-like (Figs. 1B,C, 2 F,G,J–P). One to six globular to ellipsoidal micronuclei, near, or adjacent to, macronuclear nodules, approximately 4–5 μm across in vivo. One contractile vacuole about 20–25 μm in diameter in diastole, near left margin of body about at level of cytostome (Fig. 2B). Cortical granules not present. Cytoplasm colourless, packed with numerous irregularly shaped granules (2–5 μm in size) and several food vacuoles (approx. 5–20 μm in diameter) usually present in middle region of cell, containing small flagellates and diatoms, rendering cells dark and opaque (Fig. 2A–C,F). Locomotion by moderately fast crawling on substrate or swimming around long body axis, sometimes staying immobile on substrate, with only adoral membranelles swirling .

Three large frontal cirri forming triangular pattern, one buccal cirrus, all about 35–40 μm long in vivo. Frontoventral and ventral cirri about 30–35 μm long in vivo. Invariably four frontoventral cirri with small bases; three of them (IV/3, VI/3, VI/4) almost arranged in a line, cirrus III/2 just at or slightly behind level of cirrus IV/3. Three postoral ventral cirri arranged in triangular pattern, with anterior one at or slightly in front of level of cytostome. Two relatively large pretransverse ventral cirri, the anterior one at same level as leftmost transverse cirrus. Above-mentioned cirri all positioned right of midline. Usually five transverse cirri, separated in two groups of three and two cirri, long and very broad, with cilia about 45–50 μm long in vivo, only the two right ones protruding slightly or distinctly beyond posterior end of cell (Fig. 2H,I). One left and one right marginal row, distinctly separated posteriorly, composed of about 22–30 and 27–45 cirri, respectively. Marginal cirri fine and thin compared to body size, about 20–25 μm long in vivo.

Consistently six dorsal kineties, dorsal kineties 1–3 strongly curved rightwards anteriorly, almost extending entire body length, dorsal kinety 4 slightly curved and distinctly shortened anteriorly, dorsal kineties 5 and 6 curved leftwards and slightly shortened anteriorly and posteriorly, terminating a little more anteriorly than dorsal kineties 1–4 (Fig. 1C). Dorsal bristles about 3–4 μm long in vivo (Fig. 2E). Three caudal cirri, one each at the end of dorsal kineties 1, 2, 4, widely separated, usually straight, but sometimes flexible, about 60–65 μm long (Fig. 2A–C); left caudal cirrus located just behind posterior end of left marginal row, middle one slightly right of midline, right one subterminal at right cell margin (Figs. Fig 11B, 2G).

Adoral zone of membranelles occupying 47–58% (on average 53%) of body length in protargol preparations, composed of 53–63 membranelles, commencing anteriorly near right margin of ventral surface (DE-value, distance between distal end of adoral zone of membranelles and anterior body end: adoral zone length, percentage, about 43% on average). Cilia of membranelles about 25–35 μm long in vivo. Paroral and endoral membranes parallel to each other, situated on right wall of peristome, optically crossed in some stained preparations due to flattening, both about half the length of buccal field. Paroral membrane consisting of two rows of basal bodies, almost same length as endoral membrane; endoral membrane single-rowed, extending slightly more anteriorly than paroral (Fig. 1B).

#### Deposition of specimens

Five voucher slides with protargol-stained specimens were deposited in the Laboratory of Protozoology, OUC, China, with registration numbers LXT20131105041/1–5.

### *Gastrostyla steinii* Engelmann, 1862 (Fig. 3A–N, Fig. 4A–G, Fig. 5A–F, Fig. 6A–H, Table 1)

#### Morphology of the Chinese population

Cells about 105–170 × 40–70 μm in vivo. Body semi-rigid and noncontractible. Body elliptical in outline, both ends rounded, sometimes posterior end slightly broader than ante-

**Table 1.** Morphometric characterization of *Stylonychia nodulinucleata* (upper line) and *Gastrostyla steinii* (lower line).

| Character[a] | Mean | M | SD | CV | Min | Max | *n* |
|---|---|---|---|---|---|---|---|
| Body, length | 222.2 | 220.0 | 25.5 | 11.5 | 162.0 | 261.0 | 16 |
| | 176.2 | 173.0 | 20.4 | 11.6 | 145.0 | 210.0 | 16 |
| Body, width | 121.6 | 124.0 | 14.3 | 11.8 | 90.0 | 148.0 | 16 |
| | 98.1 | 100.5 | 13.9 | 14.1 | 75.0 | 127.0 | 16 |
| Body width: length, percentage | 54.8 | 54.5 | 2.9 | 5.2 | 50.2 | 60.5 | 16 |
| | 55.6 | 56.0 | 4.3 | 7.8 | 50.0 | 64.9 | 16 |
| Body length: width, ratio | 1.8 | 1.8 | 0.1 | 5.2 | 1.7 | 2.0 | 16 |
| | 1.8 | 1.8 | 0.1 | 7.6 | 1.5 | 2.0 | 16 |
| Adoral zone length | 117.0 | 118.0 | 12.3 | 10.5 | 93.0 | 143.0 | 16 |
| | 65.4 | 67.0 | 7.1 | 10.8 | 52.0 | 75.0 | 15 |
| Adoral zone length: Body length, percentage | 52.8 | 52.6 | 3.4 | 6.4 | 46.6 | 58.1 | 16 |
| | 37.3 | 36.2 | 4.1 | 11.1 | 32.4 | 44.7 | 15 |
| Body length: Adoral zone length, ratio | 1.9 | 1.9 | 0.1 | 6.4 | 1.7 | 2.1 | 16 |
| | 2.7 | 2.8 | 0.3 | 10.5 | 2.2 | 3.1 | 15 |
| Distal end of AZM to anterior body end, distance[b] | 50.8 | 50.5 | 7.9 | 15.5 | 37.0 | 62.0 | 16 |
| DE-value[b] | 43.3 | 42.7 | 4.7 | 10.8 | 35.3 | 52.6 | 16 |
| Adoral membranelles, number | 57.2 | 57.0 | 2.8 | 4.9 | 53.0 | 63.0 | 16 |
| | 35.1 | 35.5 | 2.2 | 6.3 | 31.0 | 38.0 | 14 |
| Frontal cirri, number | 3.0 | 3.0 | 0.0 | 0.0 | 3.0 | 3.0 | 13 |
| | 3.0 | 3.0 | 0.0 | 0.0 | 3.0 | 3.0 | 16 |
| Buccal cirrus, number | 1.0 | 1.0 | 0.0 | 0.0 | 1.0 | 1.0 | 13 |
| | 1.0 | 1.0 | 0.0 | 0.0 | 1.0 | 1.0 | 16 |
| Frontoventral cirri, number[b] | 4.0 | 4.0 | 0.0 | 0.0 | 4.0 | 4.0 | 12 |
| Parabuccal cirrus, number[c] | 1.0 | 1.0 | 0.0 | 0.0 | 1.0 | 1.0 | 14 |
| Postoral ventral cirri, number | 3.0 | 3.0 | 0.0 | 0.0 | 3.0 | 3.0 | 13 |
| | 1.0 | 1.0 | 0.0 | 0.0 | 1.0 | 1.0 | 13 |
| Pretransverse ventral cirri, number | 2.0 | 2.0 | 0.0 | 0.0 | 2.0 | 2.0 | 15 |
| | 3.7 | 4.0 | 0.6 | 16.8 | 3.0 | 5.0 | 15 |
| Transverse cirri, number | 5.0 | 5.0 | 0.4 | 7.3 | 4.0 | 6.0 | 16 |
| | 4.1 | 4.0 | 0.3 | 6.2 | 4.0 | 5.0 | 16 |
| Cirri in anterior part of FVR, number[c] | 3.5 | 4.0 | 0.5 | 14.7 | 3.0 | 4.0 | 13 |
| Cirrus IV/3, number[c] | 1.0 | 1.0 | 0.0 | 0.0 | 1.0 | 1.0 | 14 |
| Cirri in posterior part of FVR, number[c] | 11.2 | 11.0 | 0.6 | 5.4 | 10.0 | 12.0 | 11 |
| Total cirri in FVR, number[c] | 15.8 | 16.0 | 0.6 | 3.8 | 15.0 | 17.0 | 11 |
| All cirri, number[c, d] | 21.3 | 21.0 | 0.8 | 3.9 | 20.0 | 23.0 | 10 |
| Left marginal cirri, number | 25.4 | 25.0 | 2.2 | 8.6 | 22.0 | 30.0 | 13 |
| | 24.9 | 25.0 | 2.4 | 9.7 | 20.0 | 28.0 | 16 |
| Right marginal cirri, number | 37.6 | 38.0 | 4.0 | 10.5 | 27.0 | 45.0 | 14 |
| | 28.3 | 28.0 | 1.9 | 6.7 | 26.0 | 32.0 | 16 |
| Caudal cirri, number | 3.0 | 3.0 | 0.0 | 0.0 | 3.0 | 3.0 | 14 |
| | 3.0 | 3.0 | 0.0 | 0.0 | 3.0 | 3.0 | 16 |
| Dorsal kineties, number | 6.0 | 6.0 | 0.0 | 0.0 | 6.0 | 6.0 | 6 |
| | 6.0 | 6.0 | 0.0 | 0.0 | 6.0 | 6.0 | 16 |
| Dikinetids in dorsal kinety 1, number[c] | 28.9 | 28.0 | 2.6 | 9.1 | 24.0 | 32.0 | 15 |
| Dikinetids in dorsal kinety 2, number[c] | 25.8 | 26.0 | 2.2 | 8.6 | 22.0 | 29.0 | 13 |
| Dikinetids in dorsal kinety 3, number[c] | 19.6 | 19.0 | 2.5 | 12.5 | 15.0 | 23.0 | 10 |
| Dikinetids in dorsal kinety 4, number[c] | 20.1 | 20.0 | 2.2 | 11.1 | 17.0 | 24.0 | 15 |
| Dikinetids in dorsal kinety 5, number[c] | 11.9 | 11.5 | 1.9 | 15.6 | 10.0 | 16.0 | 14 |
| Dikinetids in dorsal kinety 6, number[c] | 6.2 | 6.0 | 0.9 | 14.8 | 5.0 | 8.0 | 10 |
| Macronuclear nodules, number | 7.8 | 8.0 | 1.3 | 17.2 | 4.0 | 11.0 | 25 |
| | 4.0 | 4.0 | 0.0 | 0.0 | 4.0 | 4.0 | 16 |
| Anteriormost macronuclear nodule, length | 20.9 | 21.0 | 3.3 | 15.6 | 17.0 | 29.0 | 15 |
| | 29.3 | 28.0 | 3.8 | 13.0 | 23.0 | 37.0 | 16 |
| Anteriormost macronuclear nodule, width | 14.0 | 13.0 | 2.3 | 16.2 | 11.0 | 18.0 | 15 |
| | 23.4 | 23.0 | 3.8 | 16.3 | 15.0 | 30.0 | 16 |
| Posteriormost macronuclear nodule, length | 26.9 | 27.0 | 8.3 | 31.1 | 15.0 | 45.0 | 15 |
| | 23.1 | 23.0 | 3.0 | 12.9 | 17.0 | 28.0 | 16 |

Table 1 (*Continued*)

| Character[a] | Mean | M | SD | CV | Min | Max | *n* |
|---|---|---|---|---|---|---|---|
| Posteriormost macronuclear nodule, width | 13.3 | 14.0 | 2.2 | 16.5 | 9.0 | 16.0 | 15 |
| | 20.6 | 21.5 | 3.2 | 15.6 | 15.0 | 27.0 | 16 |
| Micronuclei, number | 2.9 | 3.0 | 1.4 | 47.3 | 1.0 | 6.0 | 19 |
| | 3.0 | 3.0 | 0.9 | 30.9 | 2.0 | 5.0 | 15 |

AZM, adoral zone of membranelles; CV, coefficient of variation in %; DE-value, distance between distal end of adoral zone of membranelles and anterior body end: adoral zone length, percentage; FVR, frontoventral row; M, median; Max, maximum; Mean, arithmetic mean; Min, minimum; *n*, sample number; SD, standard deviation.

[a] All data are based on protargol-stained specimens. Measurements in μm.

[b] Data for *Stylonychia nodulinucleata*.

[c] Data for *Gastrostyla steinii*.

[d] All cirri, except the frontal, buccal, transverse, marginal and caudal cirri.

rior one, margins parallel or slightly convex (Fig. 3I–K). Dorsoventrally flattened about 2:1. Four macronuclear nodules arranged in a line, positioned in midline or slightly left of it (Fig. 3B,N). Two to five micronuclei, about 4–5 μm across, attached to macronuclear nodules (Fig. 3B). One contractile vacuole about 15 μm in diameter in diastole, at about mid-body or slightly in front of it (Fig. 3N). Cytoplasm colourless, containing numerous 1–5 μm-sized, irregularly shaped crystals and shining granules (Fig. 3N). Cortical granules not present. Locomotion by slow to moderately fast crawling on substrate, occasionally swimming.

All cirri on ventral side about 20–25 μm long in life, except for the large transverse cirri with cilia about 30 μm long. Caudal cirri about 25 μm long in vivo. Invariably three frontal cirri (I/1, II/3, III/3), one buccal cirrus (II/2), one parabuccal cirrus (III/2), and one postoral ventral cir-

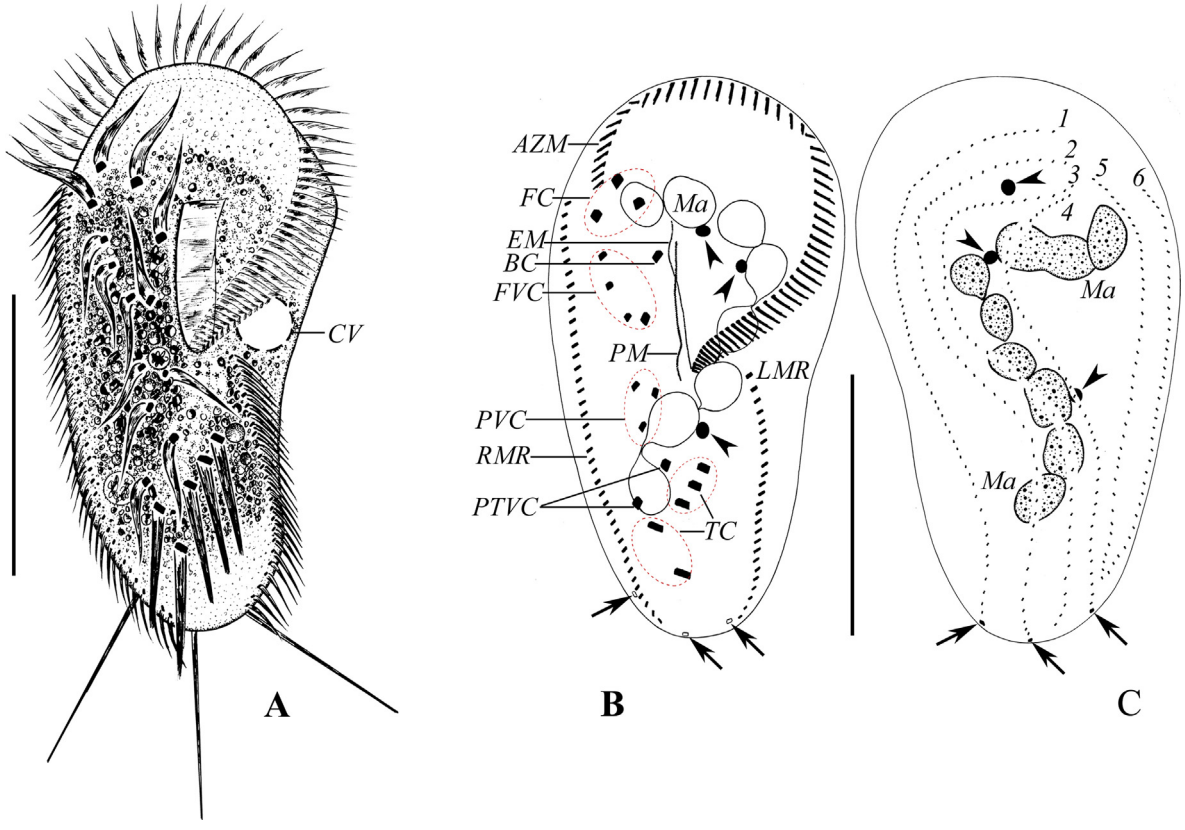


**Fig. 1.** A–C Morphology and ciliature of *Stylonychia nodulinucleata* in vivo (A) and after protargol staining (B, C). **(A)** Ventral view of a representative individual. **(B, C)** Ventral (B) and dorsal (C) views of representative specimens, showing ciliature and nuclear apparatus, arrows mark the caudal cirri, arrowheads indicate the micronuclei. AZM, adoral zone of membranelles; BC, buccal cirrus; CV, contractile vacuole; EM, endoral membrane; FC, frontal cirri; FVC, frontoventral cirri; LMR, left marginal row; Ma, macronuclear nodules; PM, paroral membrane; PTVC, pretransverse ventral cirri; PVC, postoral ventral cirri; RMR, right marginal row; TC, transverse cirri; 1–6, dorsal kineties. Scale bars = 100 μm.

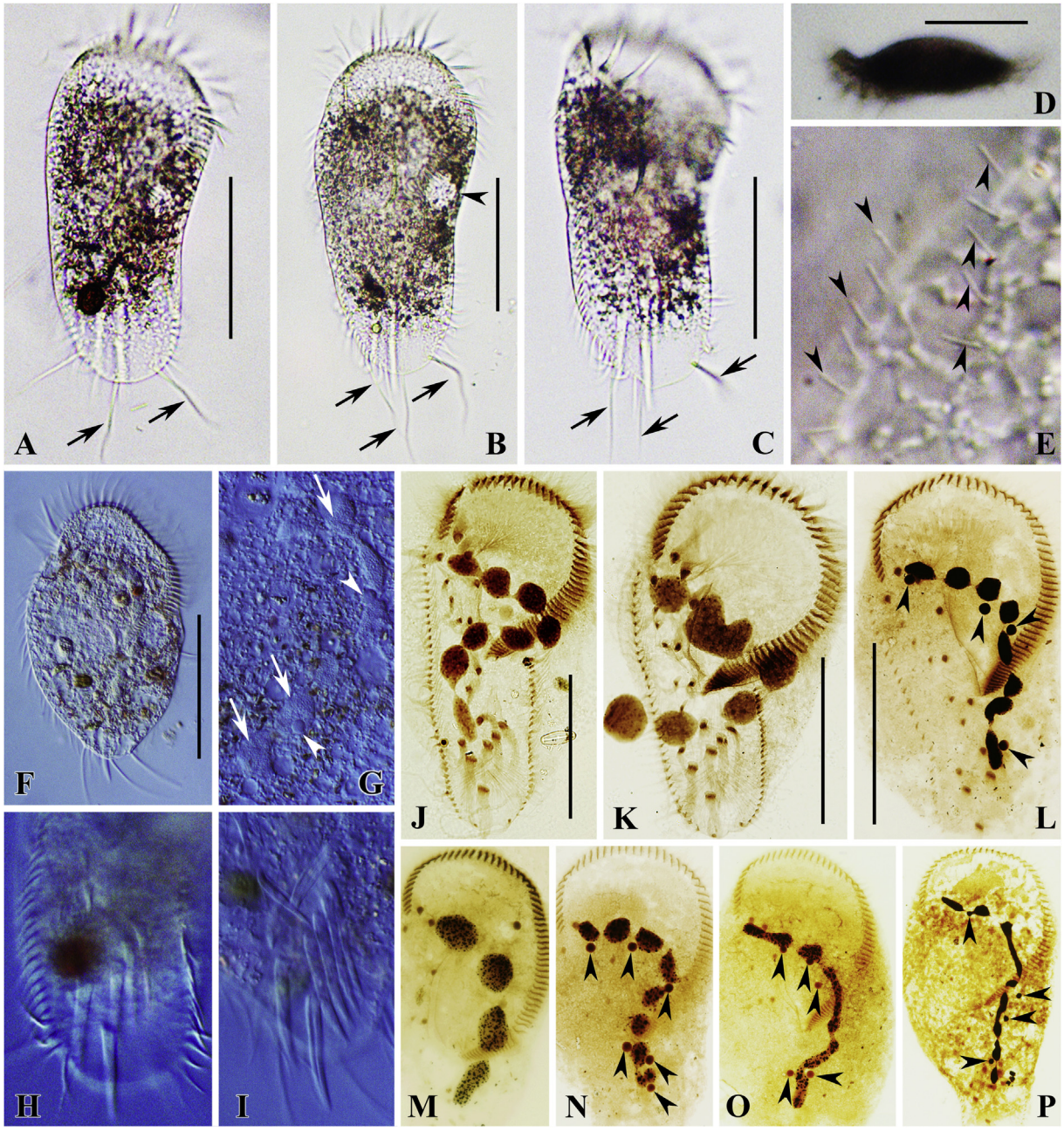


**Fig. 2.** A–P Morphology and ciliature of *Stylonychia nodulinucleata* in vivo (A–E, bright field; F–I, differential interference contrast) and after protargol staining (J–P). **(A–C)** Ventral views of representative individuals, showing body shape, contractile vacuole (arrowhead), and the long caudal cirri (arrows). **(D)** Lateral view of a representative specimen. **(E)** Dorsal bristles (arrowheads) in vivo. **(F)** Ventral view of a heavily squeezed cell, showing food vacuoles, irregularly shaped granules, and macronuclear nodules. **(G)** Portion of ventral view, showing moniliform macronucleus (arrows) and micronuclei (arrowheads). **(H, I)** Ventral views of posterior portion, showing specimens with five (H) and six (I) large transverse cirri. **(J–P)** Ventral views, showing ciliature and variations of shape and number of the macronuclear nodules, arrowheads indicate micronuclei. Scale bars = 100 μm.

rus (IV/2) (Fig. 3A,E). Frontoventral row consisting of three parts: anterior part, three or four cirri originating from frontal-ventral-transverse cirral anlage (FVTA) VI; middle part, one cirrus (IV/3); posterior part, ten to twelve cirri coming from FVTA V. Three to five, mostly four pretransverse ventral cirri originating from FVTA VI. Usually four, rarely five large transverse cirri, arranged in an oblique row, all protruding distinctly beyond posterior end of cell (Fig. 3F,M). One left and one right marginal row, nearly confluent posteriorly, with 20–28 and 26–32 cirri, respectively. Invariably six dorsal kineties, dorsal kineties 1–3 almost extending entire body length, dorsal kinety 4 only slightly shortened anteriorly, usually two dikinetids between dorsal kineties 3 and 4 (Fig. 3B,G,H, arrowheads); dorsal kineties 5 and 6 strongly

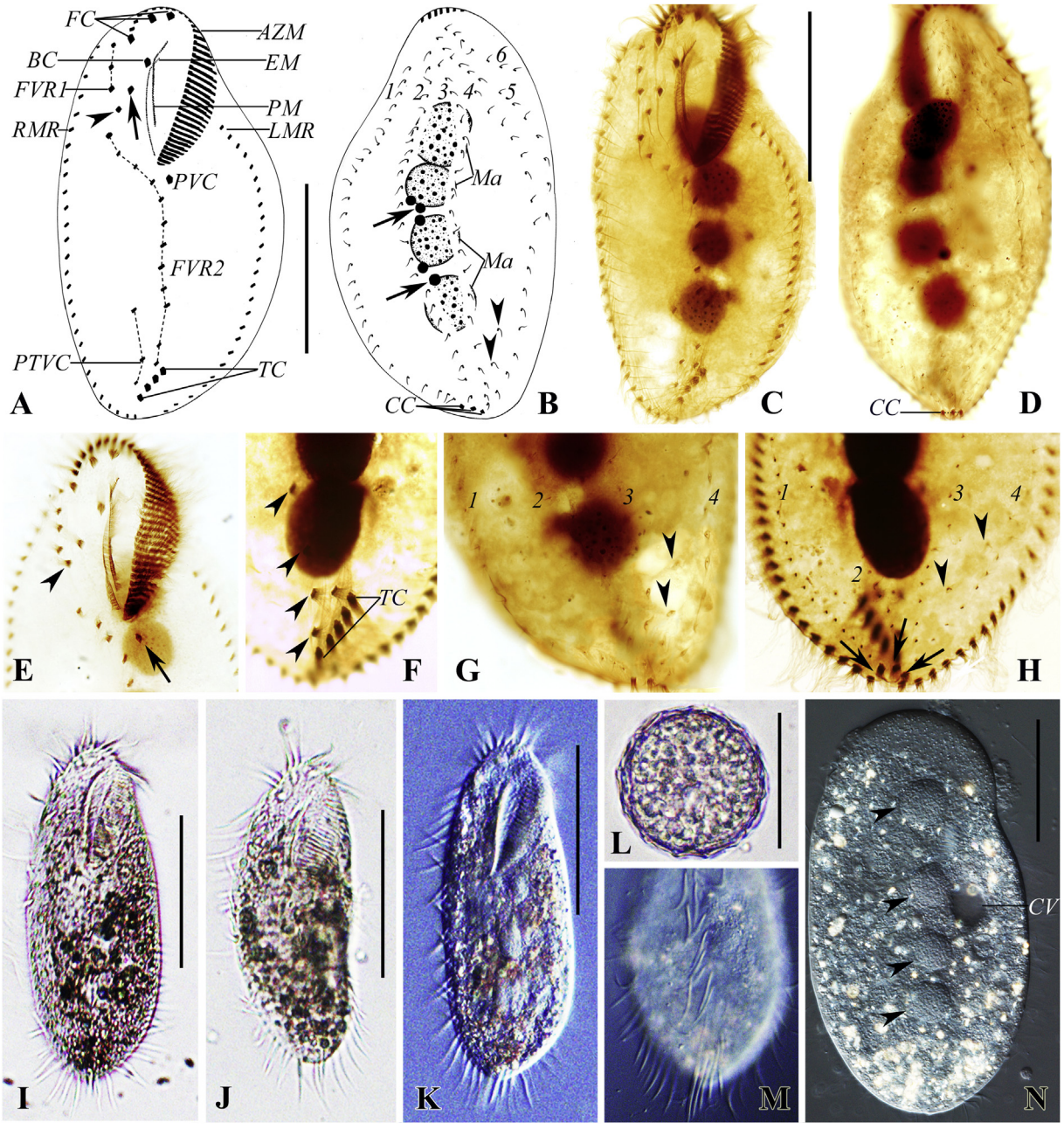


**Fig. 3.** A–N Morphology and ciliature of *Gastrostyla steinii* in vivo (I, J, L, bright field; K, M, N, differential interference contrast) and after protargol staining (A–H). **(A–D)** Ventral (A, C) and dorsal (B, D) views of representative specimens, showing ciliature and nuclear apparatus, arrow in (A) marks parabuccal cirrus, arrows in (B) mark micronuclei, arrowhead in (A) marks cirrus IV/3, arrowheads in (B) indicate dikinetids between dorsal kinety 3 and 4, hatched lines show cirri originating from the same frontal-ventral-transverse cirral anlage. **(E)** Ventral view of anterior portion, showing postoral ventral cirrus (arrow) and cirrus IV/3 (arrowhead). **(F)** Specimen with five transverse cirri and four pretransverse cirri (arrowheads) originated from frontal-ventral-transverse cirral anlage VI. **(G, H)** Dorsal views of posterior portion, showing dorsal kineties 1–4, arrowheads indicate dikinetids between dorsal kinety 3 and 4, arrows mark caudal cirri. **(I–K)** Ventral views of representative individuals. **(L)** Resting cyst, focusing on the surface. **(M)** Ventral view, showing transverse cirri protruding beyond posterior end of cell and ventral cirri aligning in a longitudinal row. **(N)** Ventral view of a heavily squeezed cell, showing contractile vacuole and four macronuclear nodules (arrowheads). AZM, adoral zone of membranelles; BC, buccal cirrus; CC, caudal cirri; CV, contractile vacuole; EM, endoral membrane; FC, frontal cirri; FVR1, anterior part of frontoventral row; FVR2, posterior part of frontoventral row; LMR, left marginal row; Ma, macronuclear nodules; PM, paroral membrane; PTVC, pretransverse ventral cirri; PVC, postoral ventral cirrus; RMR, right marginal row; TC, transverse cirri; 1–6, dorsal kineties. Scale bars = 80 μm.

shortened posteriorly (Fig. 3B,D,G,H). Dorsal bristles about 3–4 μm long in vivo. Three slightly elongated caudal cirri, one each at end of dorsal kineties 1, 2, 4, optically positioned in small gap between ends of marginal rows (Fig. 3B,D,H).

Adoral zone of membranelles occupying about 37% of body length in protargol preparations, composed of 31–38 membranelles, only four or five membranelles reaching right margin of cell. Cilia of membranelles approximately 20–25 μm long in vivo. Undulating membranes in *Oxytricha*-pattern, paroral and endoral membrane almost equal in length, optically intersecting near their anterior ends, with the former extending anteriorly to latter, paroral, consisting of two rows of basal bodies, endoral single-rowed (Fig. 3A,C,E). Resting cysts spherical, about 40–50 μm in diameter in life, with strongly wrinkled surface (Fig. 3L).

### Morphogenesis

Divisional morphogenesis commences with the formation of the oral primordium in the opisthe, which occurs as group of closely spaced basal bodies near the left transverse cirrus (Fig. 4A). Nearby parental cirri remain intact, so do not contribute to the oral primordial formation. Subsequently, with the proliferation of basal bodies, the oral primordium lengthens (Figs. 4B, 6A). Very soon, the oral primordium differentiates into new membranelles beginning at the right anterior portion and progressing posteriorly (Figs. 4C, 6 B). At the same time, anlagen I–VI of proter and opisthe are formed separately (i.e., no primary primordia present). In the proter, the parental buccal cirrus (II/2) begins to dedifferentiate into FVTA II; the parental parabuccal cirrus (III/2) contributes to the formation of FVTA III; cirrus IV/3 (perhaps together with the anteriormost cirrus of the posterior portion of the frontoventral row) forms FVTA IV–VI. In the opisthe, FVTA I–III possibly comes from the oral primordium, the postoral ventral cirrus (IV/2) contributes to the construction of FVTA IV, two cirri of parental frontoventral row form FVTA V and VI (Figs. 4C, 6B). Then, the oral primordium of the opisthe continues to form new membranelles posteriorly. Meanwhile, the parental undulating membranes dedifferentiate into the undulating membrane anlage (FVTA I) of the proter, and the left frontal cirrus is generated from the undulating membrane anlage in both dividers. All the frontal-ventral-transverse cirral anlagen lengthen to long streaks and begin to differentiate into new cirri (Figs. 4E, 6C, E). At the next stage (Figs. 4F, 6D), when the differentiation of the oral primordium is almost complete, the anterior part of the new adoral zone of membranelles curves rightwards in the opisthe. The undulating membrane anlage splits longitudinally into paroral and endoral membranes in both proter and opisthe. From the middle stage to late stage (Figs. 5 A,C,E, 6 H), the new paroral and endoral membranes are formed and arranged in *Oxytricha*-pattern. The new adoral zone of membranelles in the opisthe bends further towards the right, and the parental adoral zone is completely retained in the proter. The FVTA I–VI differentiate into new cirri in the pattern of 1: 2: 3: 3: 11–13: 7–10 from left to right and migrate to their final position in both dividers.

The marginal anlagen develop intrakinetally during the early-middle stage by dedifferentiation of the parental structures (Figs. 4E, 6C). Then, all of them lengthen towards both ends of the dividing cell (Figs. 5A,C, 6E). Finally, all marginal anlagen generate new cirri that replace the old structures (Figs. 5E, 6F).

On the dorsal side, new dorsal kineties are formed in a typical *Oxytricha*-pattern by two groups of primordia (Figs. 4D,G, 5B,D,F, 6F,G; for details, see Berger 1999; p. 73)).

Division of the nuclear apparatus proceeds in the usual way: in the early stage, replication bands are present, then all the macronuclear nodules completely fuse into a single mass, which then splits into nodules for both proter and opisthe in the late stage (Figs. 4D,G, 5B,D,F).

### Deposition of specimens

Two voucher slides with protargol-stained specimens were deposited in the Laboratory of Protozoology, OUC, China, with registration numbers LXT2015112203/1–2.

## SSU rRNA gene sequence and phylogenetic analyses (Fig. 7)

The SSU rRNA gene sequences of *Stylonychia nodulinucleata* and *Gastrostyla steinii* were deposited in GenBank database with accession numbers KY353799 and KY353800, respectively. The length and GC content of SSU rRNA gene sequences are 1723 bp and 45.10% for *Stylonychia nodulinucleata* and 1708 bp and 44.61% for *Gastrostyla steinii*, excluding primer sites.

The topologies of the ML and BI trees inferred from SSU rRNA gene sequences are generally congruent with variable support values. Therefore we present here the ML tree with bootstraps and included posterior probabilities (Fig. 7). In both analyses, *Stylonychia* (*Metastylonychia*) *nodulinucleata* is placed as a sister branch to the clade of 17 sequences within the *Stylonychia* (*Stylonychia*) *mytilus* complex (*S. mytilus*, *S. lemnae*, *S. harbinensis*, and *S. ammermanni*) with moderate to high support (ML/BI, 94%/1.00), far away from *S. notophora*. All the *Gastrostyla* sequences, except for *Gastrostyla* sp. Y2 (KT780432) (probably a misidentification), group together with moderate to high support (ML/BI, 91%/0.95) in the large group of the subfamily Stylonychinae.

# Discussion

## Comparison of *Stylonychia nodulinucleata* with other populations

Considering the body shape, the ciliature, the short undulating membranes, and the unique moniliform macronucleus, our isolate should be identified as *Stylonychia nodulinucleata*. So far, this species has been redescribed once from

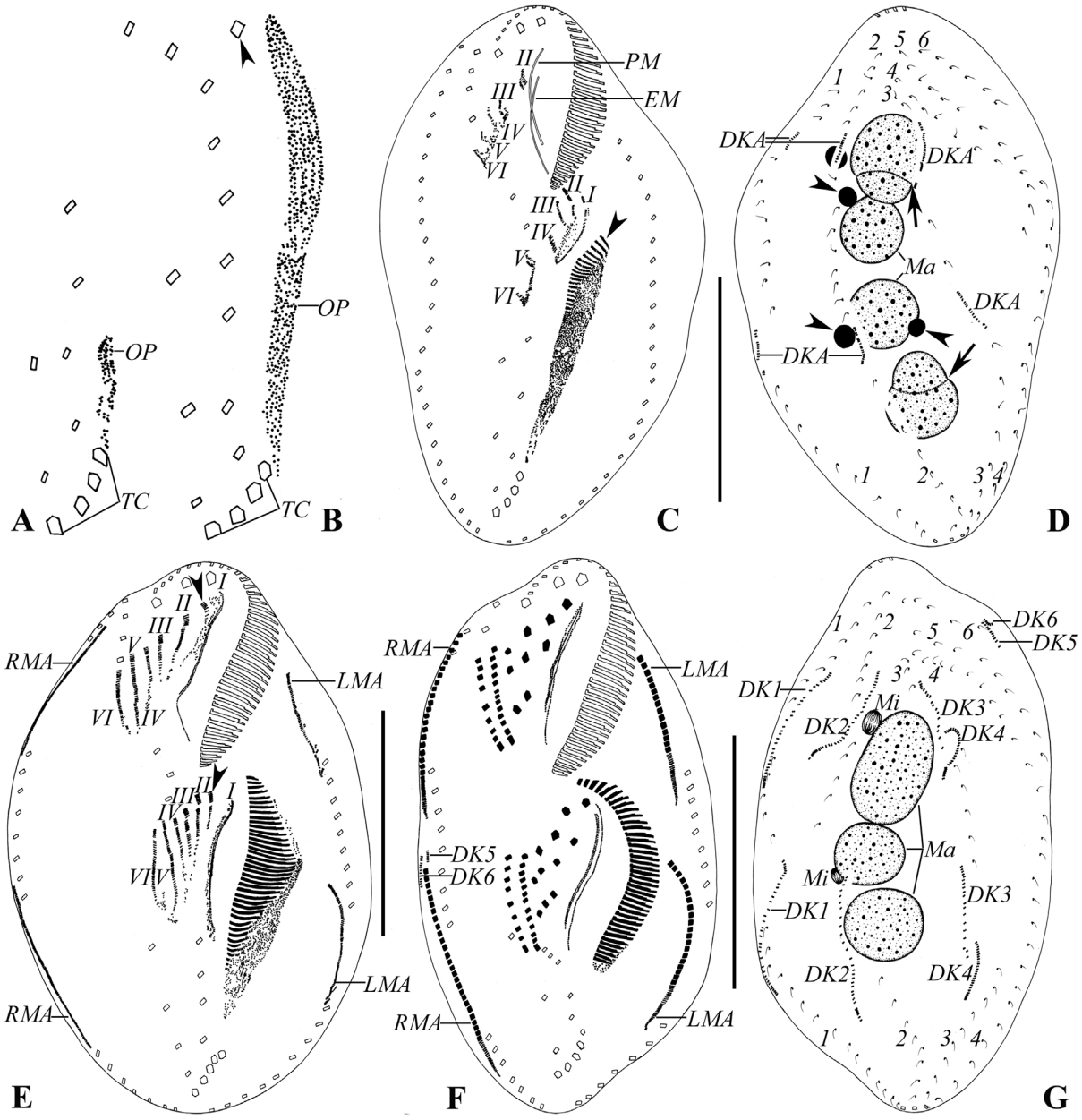


**Fig. 4.** A–G Morphogenesis of *Gastrostyla steinii* after protargol staining. **(A, B)** Ventral views of early dividers, showing oral primordium of the opisthe. **(C, D)** Ventral (C) and dorsal (D) views of the same specimen, showing the newly formed adoral membranelles (arrowhead in C), the frontal-ventral-transverse cirral anlagen dedifferentiated from parental cirri, and the dorsal kinety anlagen formed in dorsal kineties 1–3, arrows in (D) mark replication bands of macronuclear nodules, arrowheads in (D) indicate micronuclei. **(E)** Ventral view of an early-middle divider, showing the streak-like frontal-ventral-transverse cirral anlagen, the marginal anlagen, and the left frontal cirri originated from undulating membrane anlagen (arrowheads). **(F, G)** Ventral (F) and dorsal (G) views of the same middle divider, showing cirri differentiated from frontal-ventral-transverse cirral anlagen, fragmentation of dorsal kinety 3, and the newly formed dorsomarginal kineties. DKA, dorsal kinety anlagen; DK1–6, new dorsal kineties; EM, parental endoral membrane; LMA, left marginal anlagen; Ma, macronuclear nodules; Mi, micronuclei; OP, oral primordium of the opisthe; PM, parental paroral membrane; RMA, right marginal anlagen; TC, transverse cirri; I–VI, frontal-ventral-transverse cirral anlagen; 1–6, parental dorsal kineties. Scale bars = 80 μm.

Australia (Kumar and Foissner 2017). Compared with the type population isolated from marsh water of Morshan Town in Heilongjiang Province, China (Shi and Li 1993), the Zhanjiang population has a relatively smaller body size in vivo (180–240 × 80–110 μm vs. 270–310 × 95–110 μm) and fewer adoral membranelles (53–63 vs. 70–75.). However, because limnetic ciliates in different habitats can have variable body sizes, these variations can be considered as population dependent (Foissner et al. 2002). Moreover, the present population resembles the Australian one well,

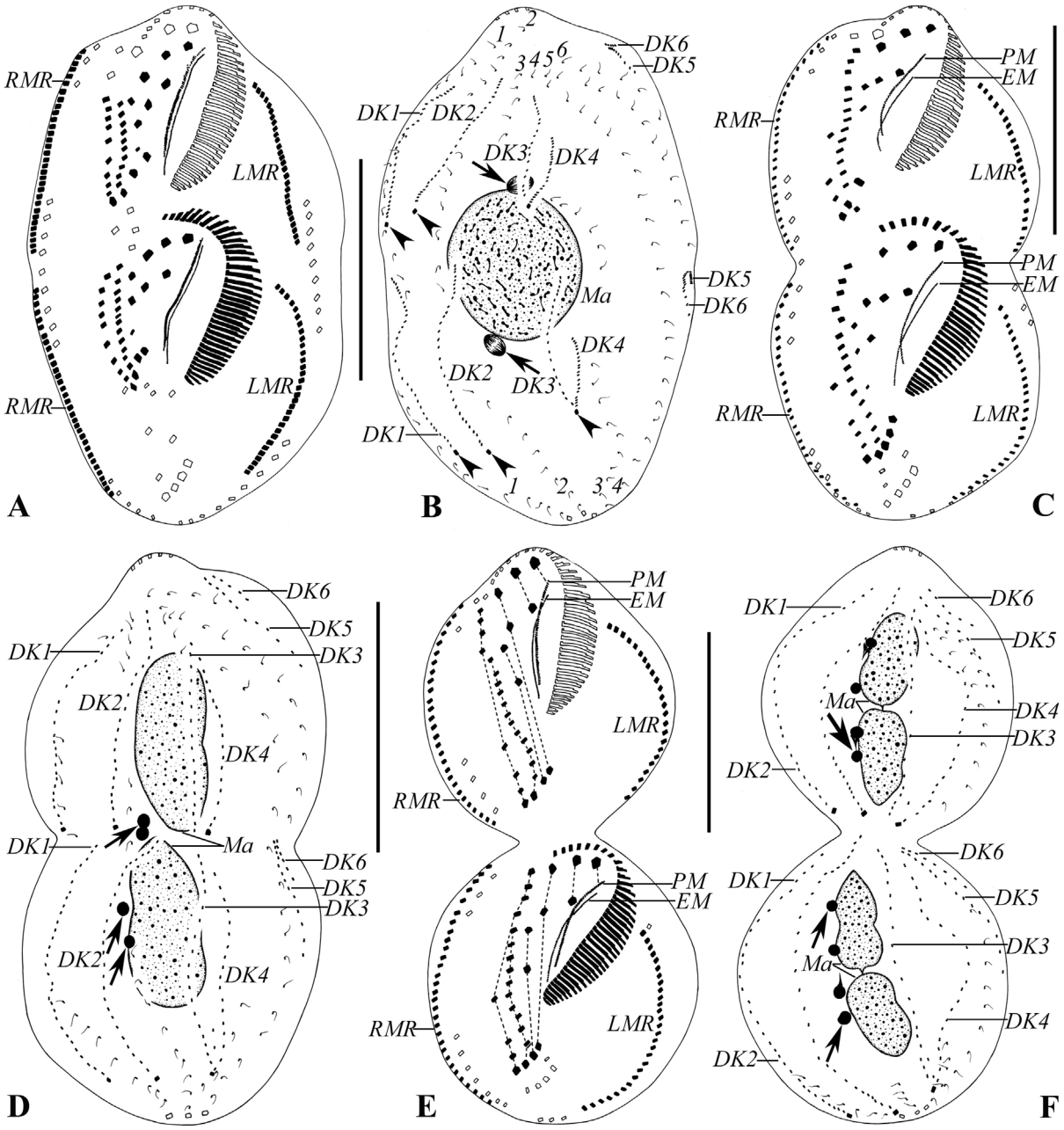


**Fig. 5.** A–F Morphogenesis of *Gastrostyla steinii* after protargol staining. **(A, B)** Ventral (A) and dorsal (B) views of the same divider, showing the newly formed caudal cirri (arrowheads) and the completely fused macronuclear mass, arrows mark the micronuclei. **(C, D)** Ventral (C) and dorsal (D) views of a middle-late divider, showing the new undulating membranes, arrows mark the micronuclei. **(E, F)** Ventral (E) and dorsal (F) views of a late divider, showing the migration of the newly formed cirri, hatched lines show cirri originating from the same frontal-ventral-transverse cirral anlage, arrows mark the micronuclei. DK1–6, new dorsal kineties; EM, new endoral membrane; LMR, left marginal row; Ma, macronuclear nodules; PM, new paroral membrane; RMR, right marginal row; 1–6, parental dorsal kineties. Scale bars = 80 μm.

for instance, in the body size (180–240 × 80–110 μm vs. 210–250 × 90–115 μm), the number of adoral membranelles (53–63 vs. 52–70), the number of left marginal cirri (22–30 vs. 24–31), the number of right marginal cirri (27–45 vs. 35–46), and the number of macronuclear nodules (on average 8 vs. 7) (Kumar and Foissner 2017).

## Biogeographic considerations of *Stylonychia nodulinucleata*

As proposed by Kumar and Foissner (2017), *Stylonychia nodulinucleata* can be considered a flagship in the ciliate world, possibly with a restricted distribution, especially because members of the *S. mytilus* complex have been inves-

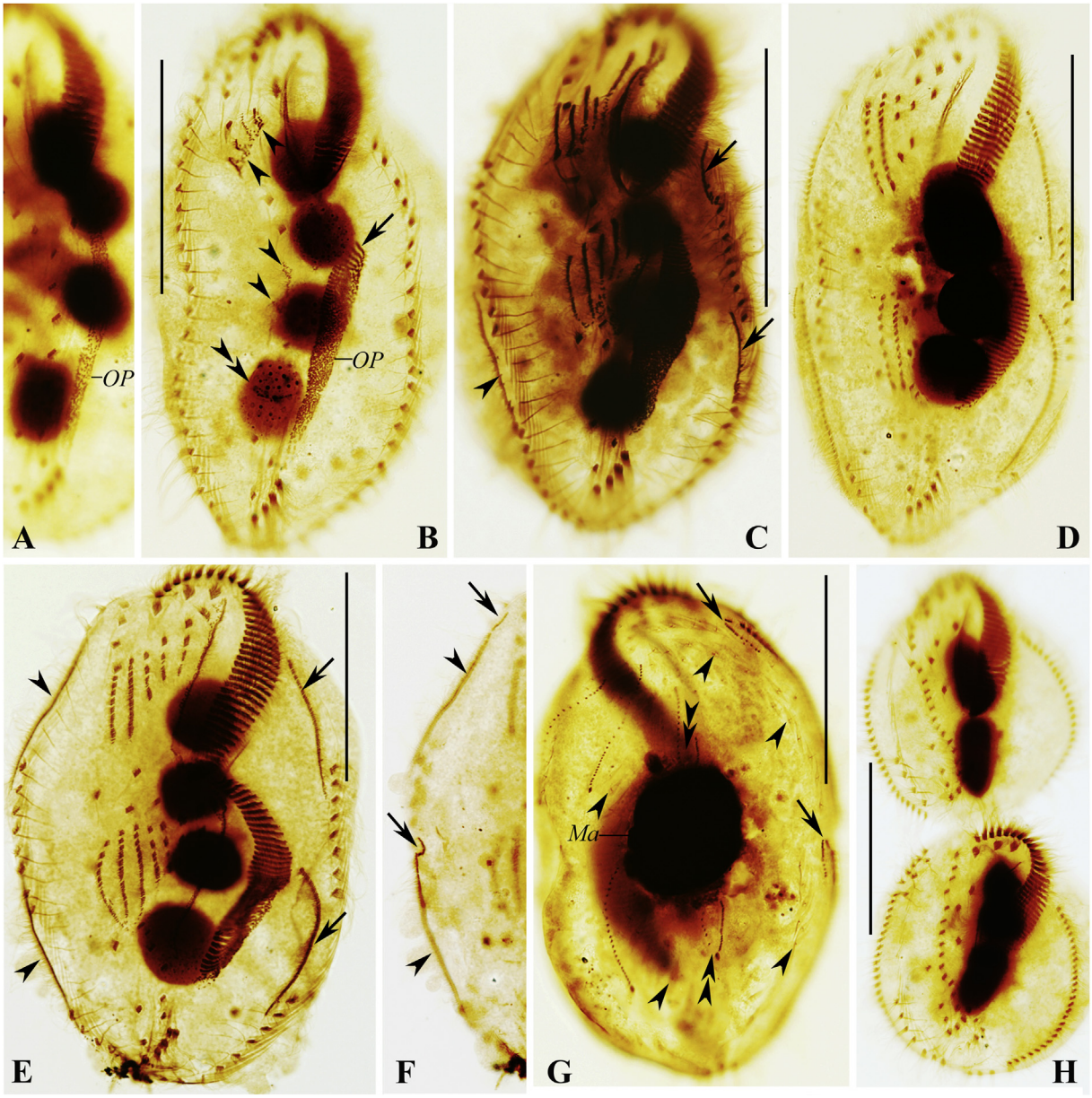


**Fig. 6.** A–H Morphogenetic photomicrographs of *Gastrostyla steinii* after protargol staining. **(A)** Ventral view of an early divider, showing oral primordium of the opisthe. **(B)** Ventral view of the same specimen as Fig. 4C, showing the newly formed adoral membranelles (arrow), the dedifferentiated parental cirri (arrowheads), and the replication band of macronuclear nodules (double arrowheads). **(C)** Ventral view of an early-middle divider, showing the streak-like frontal-ventral-transverse cirral anlagen, the left marginal anlagen (arrows), and the right marginal anlage (arrowhead). **(D)** Ventral view of the same specimen as Fig. 4F, showing cirri differentiated from frontal-ventral-transverse cirral anlagen. **(E, F)** Ventral (E) and dorsal (F) views of a divider with eight frontal-ventral-transverse cirral anlagen in the opisthe, arrowheads in (E) and (F) mark the right marginal anlagen, arrows in (E) indicate the left marginal anlagen, arrows in (F) mark the dorsomarginal anlagen fragmented from right marginal anlagen. **(G)** Dorsal view of a middle divider, showing the completely fused macronuclear mass, the newly formed dorsomarginal kineties (arrows), the fragmentation of dorsal kinety 3 (double arrowheads), and the parental dikinetids (arrowheads). **(H)** Ventral view of a late divider, showing the migration of the newly formed cirri. Ma, macronucleus; OP, oral primordium of the opisthe. Scale bars = 80 μm.

tigated intensively globally (Berger 1999). Except for the original population isolated from marsh water of North East China (the transition zone of the Holarctic; Shi and Li 1993), there are two more recent records from Maar Lake of southern China (the Tropic of the Northern Hemisphere; present paper), and almost black soil (pH 5.2) from Australia (the Tropic of the Southern Hemisphere; Kumar and Foissner 2017), suggesting a wider distribution for this species. The appearance of distributional restriction for free-living ciliates may, for the most part, reflect insufficient faunistic surveys of

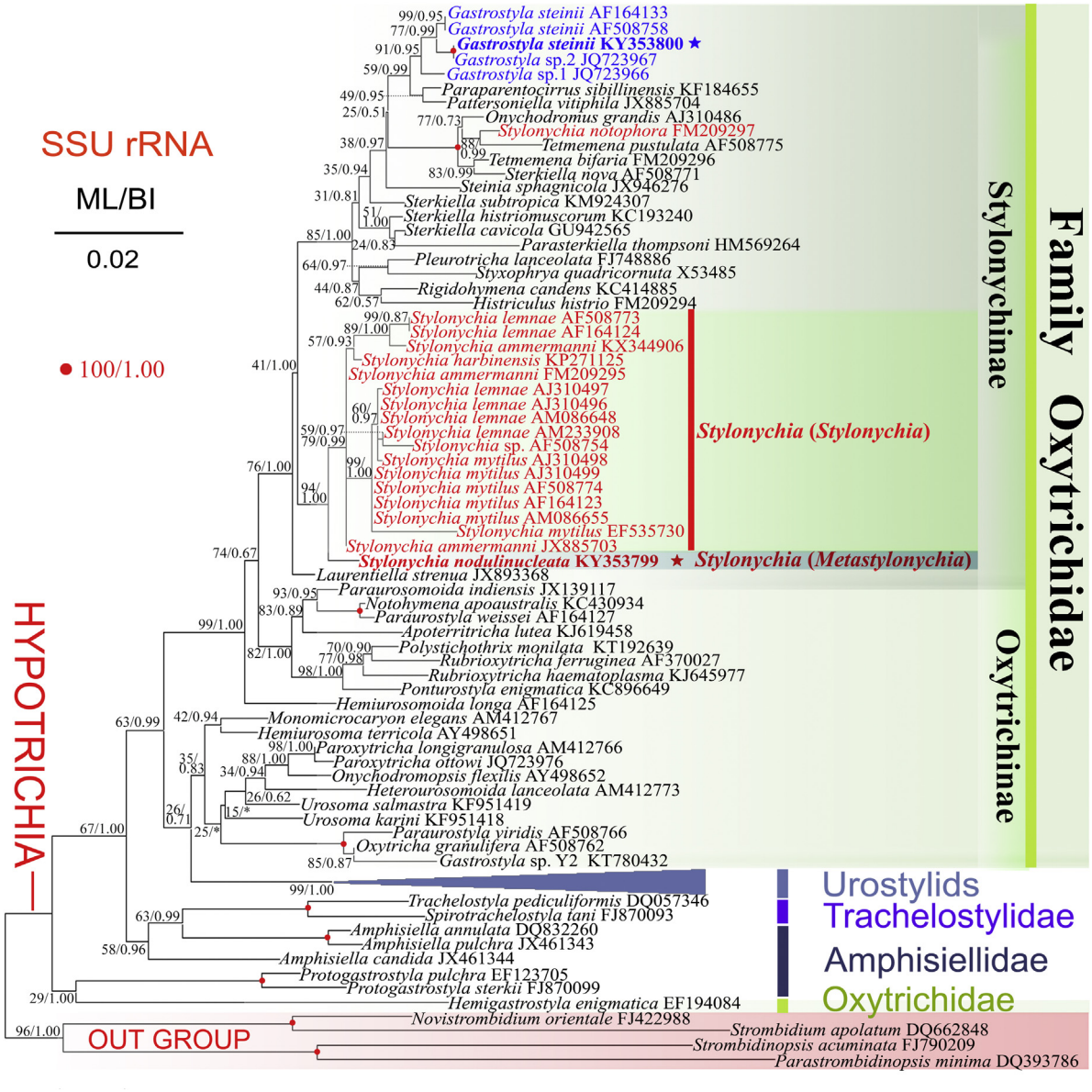


**Fig. 7.** Maximum likelihood (ML) tree inferred from the SSU rRNA gene sequences showing the systematic position of *Stylonychia nodulinucleata* and *Gastrostyla steinii* (in bold). Numbers at nodes represent the bootstrap values of maximum likelihood analysis out of 1000 replicates and the posterior probability of Bayesian analysis. "*" indicates the disagreement between BI tree and the reference ML tree. Scale bar corresponds to 2 substitutions per 100 nucleotide positions.

new habitats. That is, the trajectory of our understanding of free-living ciliate biogeography may now be from the "moderate" towards a more "minimal" endemicity model (Bass and Boenigk 2011).

## Identification of the Shenzhen population of *Gastrostyla steinii*

*Gastrostyla steinii* was first reported from Bonn, Germany in 1862 (Engelmann 1862). Subsequently, it was isolated and redescribed from freshwater and/or terrestrial habitats almost worldwide. The size of *G. steinii* reported is rather variable, from only 70 μm long up to 300 × 130 μm (Berger 1999; Foissner et al. 2002). The Shenzhen population is about 105–170 × 40–70 μm in vivo, which is in the range of body size described. Apart from slight differences in the number of frontoventral and pretransverse ventral cirri, the Shenzhen population corresponds well with the previous descriptions in diagnostic features (body shape, infraciliature, morphogenetic features, and four macronuclear nodules), and matches, especially well, the population described by Foissner et al. (2002), even with regard to the number of frontoventral and pretransverse ventral cirri, thus the species identification is not in doubt.

### Morphogenetic comparison of *Gastrostyla steinii* among populations

Detailed data on the ontogenesis of *Gastrostyla steinii* were published by Walker and Grim (1973), Hemberger (1982) and Foissner et al. (2002). Most ontogenetic events of the Shenzhen population agree well with previous studies, especially the origination of the frontal-ventral-transverse cirral anlagen (FVTA), which confirms the stability of morphogenetic process. The minor difference is that more cirri originate from FVTA V and VI in our population compared with others. This leads to more cirri in the frontoventral row and more pretransverse cirri. In this work, we give information on the fate of the parental dorsal row dikinetids, only several of those in dorsal kineties 1–3 contribute to the formation of dorsal kinety anlagen, most of them being retained unchanged until the middle-late stage.

### Phylogenetic analyses of *Stylonychia*

Berger (1999) included eleven species within the genus *Stylonychia*; three of which have been transferred to *Tetmemena*, viz., *T. pustulata*, *T. bifaria*, and *T. vorax* (Berger 2001; Eigner 1997, 1999). Since then, four more species have been added to the genus *Stylonychia*, viz., *S. ammermanni*, *S. gibbera*, *S. notophorides*, and *S. harbinensis* (very likely a synonym of *S. ammermanni*) (Foissner 2016; Gupta et al. 2001; Shi and Ammermann 2004). However, several of the 12 species assigned to *Stylonychia*, so far, possibly belong to the genus *Tetmemena*, which is also proposed by previous studies (Kumar and Foissner 2017; Kumar et al. 2016). In addition, Kumar and Foissner (2017) proposed to divide the genus *Stylonychia* into two subgenera, *S.* (*Stylonychia*), and *S.* (*Metastylonychia*), mainly based on the macronuclear feature and the ontogenetic information. This is supported by the phylogenetic analyses (Fig. 7), all the sequences of the *S.* (*S.*) *mytilus* complex (*S.* (*S.*) *ammermanni*, *S.* (*S.*) *harbinensis*, *S.* (*S.*) *lemnae*, and *S.* (*S.*) *mytilus*) clustering in a clade (ML/BI, 79%/0.99), which is placed as a sister group to *S.* (*Metastylonychia*) *nodulinucleata* with moderate to high support (ML/BI, 94%/1.00). The phylogenetic trees show that *S.* (*S.*) *notophora* (no morphological data are available for this population, and misidentification cannot be excluded) groups together with *Tetmemena pustulata*, instead of with other *Stylonychia* species. This placement also agrees well with the morphological evidence. All the species of the *S.* (*S.*) *mytilus* complex and *S.* (*Metastylonychia*) *nodulinucleata* share the following features, different from *S. notophora*, features of which are similar to *Tetmemena* species: (1) body outline obovate, with anterior end broadly rounded or obliquely truncated vs. body outline elliptical; (2) three caudal cirri widely spaced vs. caudal cirri narrowly spaced; (3) dorsal kineties 1–4 more or less distinctly curved rightwards anteriorly vs. not curved (Berger 1999; Gupta et al. 2001; Kumar and Foissner 2017; Kumar et al. 2016; Shi and Ammermann 2004).

### Monophyly and phylogenetic position of the genus *Gastrostyla*

Berger (1999) treated *Gastrostyla*, including eight species, as a genus of unclear position within the family Oxytrichidae. Now, with several of them transferred to other genera and more species added, *Gastrostyla* is a genus with six species included (Berger 2008; Foissner 2016; Foissner et al. 2002, 2004; Gong et al. 2007; Song and Wilbert 1997; Xu et al. 2000). So far, only the sequences for the type species, *Gastrostyla steinii*, and three unidentified *Gastrostyla* species are available. In our phylogenetic analyses, five *Gastrostyla* spp. form a moderately to highly supported clade (ML/BI, 91%/0.95) within the subfamily Stylonychinae. However, *Gastrostyla* sp. Y2 (KT780432) with no morphological information available, very likely a misidentification, groups with *Oxytricha granulifera* in the subfamily Oxytrichinae.

So far, *Gastrostyla* appears to be a monophyletic group of the subfamily Stylonychinae, consistent with the morphologic and morphogenetic features (body rigid/semi-rigid, cortical granules lacking, dorsal morphogenesis in *Oxytricha* pattern). However, as proposed by Foissner et al. (2002, 2004), *Gastrostyla* may be paraphyletic because of rather conspicuous morphological and ontogenetic differences in the individual species. Thus, the confirmation of the monophyly of *Gastrostyla* needs additional molecular information of other species.

## Acknowledgements

This work was supported by the National Natural Science Foundation of China (Project numbers: 41576134, 31430077, 41576148), the China Scholarship Council, and the National Research Foundation of Korean government of MOE and MSIP (2015R1D1A09058911, 2015H1D3A1062066). Thanks are due to Prof. Weibo Song (OUC) for critically reading the drafts and providing helpful suggestions. We also thank our colleagues, Mr. Zhishuai Qu and Mingjian Liu (OUC) for their generous help with collecting samples.

## References

Adl, S.M., Simpson, A.G.B., Lane, C.E., Lukeš, J., Bass, D., Bowser, S.S., Brown, M.W., Burki, F., Dunthorn, M., Hampl, V., Heiss, A., Hoppenrath, M., Lara, E., Gall, L.L., Lynn, D.H., Mcmanus, H., Mitchell, E.A.D., Mozley-Stanridge, S.E., Parfrey, L.W., Pawlowski, J., Rueckert, S., Shadwick, L., Schoch, C.L., Smirnov, A., Spiegel, F.W., 2012. The revised classification of eukaryotes. J. Eukaryot. Microbiol. 59, 429–493.

Alfaro, M.E., Zoller, S., Lutzoni, F., 2003. Bayes or bootstrap? A simulation study comparing the performance of

Bayesian Markov chain Monte Carlo sampling and bootstrapping in assessing phylogenetic confidence. Mol. Biol. Evol. 20, 255–266.

Bass, D., Boenigk, J., 2011. Everything is everywhere: a twenty-first century de-/reconstruction with respect to protists. In: Fontaneto, D. (Ed.), Biogeography of Microscopic Organisms: Is Everything Small Everywhere? Cambridge University Press, pp. 88–110.

Berger, H., 1999. Monograph of the Oxytrichidae (Ciliophora, Hypotrichia). Monogr. Biol. 78, 1–1080.

Berger, H., 2001. Catalogue of Ciliate Names 1. Hypotrichs. Verlag Helmut Berger, Salzburg.

Berger, H., 2008. Monograph of the Amphisiellidae and Trachelostylidae (Ciliophora, Hypotricha). Monogr. Biol. 88, 1–737.

Berger, H., 2011. Monograph of the Gonostomatidae and Kahliellidae (Ciliophora, Hypotricha). Monogr. Biol. 90, 1–741.

Chen, L., Zhao, X., Ma, H., Warren, A., Shao, C., Huang, J., 2015. Morphology, morphogenesis and molecular phylogeny of a soil ciliate, *Pseudouroleptus caudatus caudatus* Hemberger, 1985 (Ciliophora, Hypotricha), from Lhalu Wetland, Tibet. Eur. J. Protistol. 51, 1–14.

Edgar, R.C., 2004. MUSCLE: multiple sequence alignment with high accuracy and high throughput. Nucleic Acids Res. 32, 1792–1797.

Ehrenberg, C.G., 1830. Beiträge zur Kenntniß der Organisation der Infusorien und ihrer geographischen Verbreitung besonders in Sibirien. Abh. Akad. Wiss. Berlin, 1–88.

Eigner, P., 1997. Evolution of morphogenetic processes in the Orthoamphisiellidae n. fam., Oxytrichidae, and Parakahliellidae n. fam., and their depiction using a computer method (Ciliophora, Hypotrichida). J. Eukaryot. Microbiol. 44, 553–573.

Eigner, P., 1999. Comparison of divisional morphogenesis in four morphologically different clones of the genus *Gonostomum* and update of the natural hypotrich system (Ciliophora, Hypotrichida). Eur. J. Protistol. 35, 34–48.

Engelmann, T.W., 1862. Zur Naturgeschichte der Infusionsthiere. Z. Wiss. Zool. 11, 347–393.

Fan, Y., Zhao, X., Hu, X., Miao, M., Warren, A., Song, W., 2015. Taxonomy and molecular phylogeny of two novel ciliates, with establishment of a new genus, *Pseudogastrostyla* n. g. (Ciliophora, Hypotrichia, Oxytrichidae). Eur. J. Protistol. 51, 374–385.

Foissner, W., 2016. Terrestrial and semiterrestrial ciliates (Protozoa, Ciliophora) from Venezuela and Galápagos. Denisia 35, 1–912.

Foissner, W., Agatha, S., Berger, H., 2002. Soil ciliates (Protozoa, Ciliophora) from Namibia (Southwest Africa), with emphasis on two contrasting environments, the Etosha region and the Namib Desert. Denisia 5, 1–1459.

Foissner, W., Moon-van der Staay, S.Y., van der Staay, G.W.M., Hackstein, J.H.P., Krautgartner, W.D., Berger, H., 2004. Reconciling classical and molecular phylogenies in the stichotrichines (Ciliophora Spirotrichea), including new sequences from some rare species. Eur. J. Protistol. 40, 265–281.

Fromentel, E.de, 1875. Études sur les microzoaires ou infusoires proprement dits comprenent de nouvelles recherches sur leur organisation, leur classification et la description des espèces nouvelles ou peu connus. G. Masson, Paris, pp. 89–192.

Gao, F., Warren, A., Zhang, Q., Gong, J., Miao, M., Sun, P., Xu, D., Huang, J., Yi, Z., Song, W., 2016. The all-data-based evolutionary hypothesis of ciliated protists with a revised classification of the phylum Ciliophora (Eukaryota, Alveolata). Sci. Rep. 6, 24874.

Gong, J., Kim, S., Kim, S., Min, G., Roberts, D., Warren, A., Choi, J., 2007. Taxonomic redescriptions of two ciliates, *Protogastrostyla pulchra* n. g., n. comb. and *Hemigastrostyla enigmatica* (Ciliophora, Spirotrichea Stichotrichia), with phylogenetic analyses based on 18S and 28S rRNA gene sequences. J. Eukaryot. Microbiol. 54, 468–478.

Gouy, M., Guindon, S., Gascuel, O., 2010. SeaView version 4: a multiplatform graphical user interface for sequence alignment and phylogenetic tree building. Mol. Biol. Evol. 27, 221–224.

Gupta, R., Kamra, K., Arora, S., Sapra, G.R., 2001. *Stylonychia ammermanni* sp. n., a new oxytrichid (Ciliophora: Hypotrichida) ciliate from the river Yamuna, Delhi, India. Acta Protozool. 40, 75–82.

Hall, T.A., 1999. BioEdit: a user-friendly biological sequence alignment editor and analysis program for Windows 95/98/NT. Nucleic Acids Symp. 41, 95–98.

Hemberger, H., 1982. Revision der Ordnung Hypotrichida Stein (Ciliophora Protozoa) an Hand von Protargolpräparaten und Morphogenesedarstellungen. Dissertation Universität Bonn.

Hillis, D.M., Bull, J.J., 1993. An empirical test of bootstrapping as a method for assessing confidence in phylogenetic analysis. Syst. Biol. 42, 182–192.

Hu, X., Kusuoka, Y., 2015. Two oxytrichids from the ancient Lake Biwa, Japan, with notes on morphogenesis of *Notohymena australis* (Ciliophora, Sporadotrichida). Acta Protozool. 54, 107–122.

Jung, J.H., Park, K.M., Min, G.S., 2015. Morphology and molecular phylogeny of *Pseudocyrtohymena koreana* n. g., n. sp. and Antarctic *Neokeronopsis asiatica* Foissner, et al., 2010 (Ciliophora, Sporadotrichida), with a brief discussion of the *Cyrtohymena* undulating membranes pattern. J. Eukaryot. Microbiol. 62, 280–297.

Kumar, S., Foissner, W., 2017. Morphology and ontogenesis of *Stylonychia* (*Metastylonychia*) *nodulinucleata* nov. subgen. (Ciliophora, Hypotricha) from Australia. Eur. J. Protistol. 57, 61–72.

Kumar, S., Kamra, K., Bharti, D., Terza, A.L., Sehgal, N., Warren, A., Sapra, G.R., 2015. Morphology, morphogenesis, and molecular phylogeny of *Sterkiella tetracirrata* n. sp. (Ciliophora Oxytrichidae), from the Silent Valley National Park, India. Eur. J. Protistol. 51, 86–97.

Kumar, S., Bharti, D., Quintela-Alonso, P., Shin, M.K., Terza, A.L., 2016. Fine-tune investigations on three stylonychid (Ciliophora, Hypotricha) ciliates. Eur. J. Protistol. 56, 200–218.

Lu, X., Shao, C., Yu, Y., Warren, A., Huang, J., 2015. Reconsideration of the 'well-known' hypotrichous ciliate *Pleurotricha curdsi* (Shi, et al., 2002) Gupta et al., 2003 (Ciliophora, Sporadotrichida), with notes on its morphology, morphogenesis and molecular phylogeny. Int. J. Syst. Evol. Microbiol. 65, 3216–3225.

Lynn, D.H., 2008. The Ciliated Protozoa: Characterization, Classification, and Guide to the Literature, third edition. Springer Press, New York.

Medlin, L., Elwood, H.J., Stickel, S., Sogin, M.L., 1988. The characterization of enzymatically amplified eukaryotes 16S-like ribosomal RNA coding regions. Gene 71, 491–500.

Miller, M.A., Pfeiffer, W., Schwartz, T., 2010. Creating the CIPRES Science Gateway for inference of large phylogenetic trees. In:

Proceedings of the Gateway Computing Environments Workshop (GCE), New Orleans, Louisiana, pp. 1–8.

Nylander, J.A.A., 2004. MrModeltest 2.2. Program distributed by the author. Evolutionary Biology Centre, Uppsala University, Uppsala, Sweden.

Ronquist, F., Teslenko, M., van der Mark, P., Ayres, D.L., Darling, A., Höhna, S., Larget, B., Liu, L., Suchard, M.A., Huelsenbeck, J.P., 2012. MrBayes 3.2: efficient Bayesian phylogenetic inference and model choice across a large model space. Syst. Biol. 61, 539–542.

Sela, I., Ashkenazy, H., Katoh, K., Pupko, T., 2015. GUIDANCE2: accurate detection of unreliable alignment regions accounting for the uncertainty of multiple parameters. Nucl. Acids Res. 43, W7–W14.

Shao, C., Song, W., Al-Rasheid, K.A.S., Berger, H., 2011. Redefinition and reassignment of the 18-cirri genera *Hemigastrostyla*, *Oxytricha*, *Urosomoida*, and *Actinotricha* (Ciliophora, Hypotricha), and description of one new genus and two new species. Acta Protozool. 50, 263–287.

Shao, C., Chen, L., Pan, Y., Warren, A., Miao, M., 2014a. Morphology and phylogenetic position of the oxytrichid ciliates, *Urosoma salmastra* (Dragesco and Dragesco-Kernéis, 1986) Berger, 1999 and *U. karinae sinense* nov. sspec. (Ciliophora, Hypotrichia). Eur. J. Protistol. 50, 593–605.

Shao, C., Lv, Z., Pan, Y., Al-Rasheid, K.A.S., Yi, Z., 2014b. Morphology and phylogenetic analysis of two oxytrichid soil ciliates from China, *Oxytricha paragranulifera* n. sp. and *Oxytricha granulifera* Foissner and Adam, 1983 (Protista, Ciliophora, Hypotrichia). Int. J. Syst. Evol. Microbiol. 64, 3016–3027.

Shao, C., Lu, X., Ma, H., 2015. A general overview of the typical 18 frontal-ventral-transverse cirri Oxytrichidae s. l. genera (Ciliophora, Hypotrichia). J. Ocean Univ. China 14, 522–532.

Shi, X., Ammermann, D., 2004. *Stylonychia harbinensis* sp. n. a new oxytrichid ciliate (Ciliophora, Hypotrichia) from the Heilongjiang Province, China. Protistology 3, 219–222.

Shi, X., Li, H., 1993. Discovery of *Stylonychia nodulinucleata* sp. nov. (Ciliophora Hypotrichida, Oxytrichidae) and comparison of its neighboring species. Zool. Res. 14, 10–14.

Singh, J., Kamra, K., 2015. Molecular phylogeny of *Urosomoida agilis*, and new combinations: *Hemiurosomoida longa* gen. nov. comb. nov., and *Heterourosomoida lanceolata* gen. nov., comb. nov. (Ciliophora, Hypotricha). Eur. J. Protistol. 51, 55–65.

Singh, J., Kamra, K., Sapra, G.R., 2013. Morphology, ontogenesis, and molecular phylogeny of an Indian population of *Cyrtohymena* (*Cyrtohymenides*) *shii*, including remarks on the subgenus. Eur. J. Protistol. 49, 283–297.

Song, W., Wilbert, N., 1997. Morphological investigations on some free living ciliates (Protozoa, Ciliophora) from China Sea with description of a new hypotrichous genus *Hemigastrostyla* n. g. Arch. Protistenkd. 148, 413–444.

Song, W., Warren, A., Hu, X., 2009. Free-Living Ciliates in the Bohai and Yellow Seas, China. Science Press, Beijing.

Stamatakis, A., Hoover, P., Rougemont, J., 2008. A rapid bootstrap algorithm for the RAxML web-servers. Syst. Biol. 75, 758–771.

Tamura, K., Stecher, G., Peterson, D., Filipski, A., Dudley, J., Kumar, S., 2013. MEGA6: molecular evolutionary genetics analysis version 6.0. Mol. Biol. Evol. 30, 2725–2729.

Walker, G.K., Grim, J.N., 1973. Morphogenesis and polymorphism in *Gastrostyla steinii*. J. Protozool. 20, 566–573.

Wang, J., Lyu, Z., Warren, A., Wang, F., Shao, C., 2016. Morphology, ontogeny and molecular phylogeny of a novel saline soil ciliate, *Urosomoida paragiliformis* n. sp. (Ciliophora, Hypotrichia). Eur. J. Protistol. 56, 79–89.

Wilbert, N., 1975. Eine verbesserte Technik der Protargolimprägnation für Ciliaten. Mikrokosmos 64, 171–179.

Xu, Z., Shi, X., Shi, X., 2000. Morphology and morphogenesis of *Gastrostyla opisthoclada* sp. nov. (Ciliophora: Hypotrichida). Acta Zootaxon. Sin. 25, 268–274.

Zhao, X., Gao, S., Fan, Y., Strueder-Kypke, M., Huang, J., 2015. Phylogenetic framework of the systematically confused *Anteholosticha-Holosticha* complex (Ciliophora, Hypotrichia) based on multigene analysis. Mol. Phylogenet. Evol. 91, 238–247.